

## Functional and Structural Analysis of ClC-K Chloride Channels Involved in Renal Disease\*

Received for publication, March 9, 2000, and in revised form, May 25, 2000  
Published, JBC Papers in Press, May 30, 2000, DOI 10.1074/jbc.M001987200

Siegfried Waldegger‡ and Thomas J. Jentsch

From the Zentrum für Molekulare Neurobiologie, University of Hamburg, Martinistr. 85, D-20246 Hamburg, Germany

ClC-K channels belong to the CLC family of chloride channels and are predominantly expressed in the kidney. Genetic evidence suggests their involvement in transepithelial transport of chloride in distal nephron segments; ClC-K1 gene deletion leads to nephrogenic diabetes insipidus in mice, and mutations of the hClC-Kb gene cause Bartter's syndrome type III in humans. Expression of rClC-K1 in *Xenopus* oocytes yielded voltage-independent currents that were pH-sensitive, had a  $\text{Br}^- > \text{NO}_3^- = \text{Cl}^- > \text{I}^-$  conductance sequence, and were activated by extracellular calcium. A glutamate for valine exchange at amino acid position 166 induced strong voltage dependence and altered the conductance sequence of ClC-K1. This demonstrates that rClC-K1 indeed functions as an anion channel. By contrast, we did not detect currents upon hClC-Kb expression in *Xenopus* oocytes. Using a chimeric approach, we defined a protein domain that, when replaced by that of rClC-K1, allowed the functional expression of a chimera consisting predominantly of hClC-Kb. Its currents were linear and were inhibited by extracellular acidification. Contrasting with rClC-K1, they displayed a  $\text{Cl}^- > \text{Br}^- > \text{I}^- > \text{NO}_3^-$  conductance sequence and were not augmented by extracellular calcium. Insertion of point mutations associated with Bartter's syndrome type III destroyed channel activity. We conclude that ClC-K proteins form constitutively open chloride channels with distinct physiological characteristics.

The closely related ClC-K proteins belong to the CLC family of chloride channels (1). They are nearly exclusively expressed in the kidney. Two isoforms have been identified that were termed hClC-Ka and hClC-Kb in humans (2) and rClC-K1 and rClC-K2 in rats (the lowercase prefix indicates the species) (2–4). The high degree of identity (>90%) between the two human ClC-K isoforms makes a correlation with the corresponding mouse and rat counterparts difficult. ClC-K genes were also cloned from rabbit (ocClC-Ka) (5) and *Xenopus* (xClC-K) (6). Whereas the expression of rClC-K1 protein may be confined to the ascending thin limb of Henle's loop (7), rClC-K2 appears to be expressed in several nephron segments. Depending on the antibodies used, several studies differ somewhat as to the localization to different nephron segments. A common finding, however, is the expression of rClC-K2 (and

ocClC-Ka) at the basolateral side of the thick ascending limb and other more distally located nephron segments (8, 9). Together with the ascending thin limb, these nephron segments are the main site of transcellular chloride reabsorption. They reabsorb about 30% of the chloride that is filtered at the glomeruli and thereby play an important role in the maintenance of body salt and fluid balance. The expression pattern suggests that ClC-K proteins are involved in transcellular chloride transport. This notion is strongly supported by two genetic findings. First, disruption of the *CLCNK1* gene (coding for ClC-K1) in mice induces nephrogenic diabetes insipidus (10). This is presumably due to a urinary concentration defect caused by a reduced medullary salt concentration. Second, mutations in the hClC-Kb gene (*CLCNKB*) are associated with Bartter's syndrome (11). This autosomal recessive salt-wasting disorder is characterized by a reduced sodium chloride reabsorption in the thick ascending limb. This puts hClC-Kb into a functional relationship with the apical NaK2Cl cotransporter and with the ROMK potassium channel, whose inactivation causes other variants of Bartter's syndrome (12, 13). These findings are compatible with a transport model in which chloride is taken up apically by the cotransporter (the potassium is recycled over the apical membrane by ROMK) and then leaves the cell at the basolateral membrane via hClC-Kb channels.

The different phenotypes observed upon mutations in mClC-K1 and hClC-Kb may indicate that mClC-K1 is the homologue of hClC-Ka rather than of hClC-Kb. Both phenotypes may be explained by a loss of plasma membrane chloride transport. However, heterologous expression of ClC-K proteins yielded controversial results. Uchida *et al.* reported that expression of rat ClC-K1 in *Xenopus* oocytes induced outwardly rectifying chloride currents that resembled those observed in the ascending thin limb (7). These currents are inhibited by acidic extracellular pH or by reducing the extracellular calcium concentration, and have an anion conductivity sequence of  $\text{Br}^- > \text{Cl}^- > \text{I}^-$  (4). Although initially we could not reproduce these results (2), with an optimized vector we now succeeded in expressing rClC-K1 with similar properties. However, with the same expression vector we could not detect currents upon expression of rClC-K2, hClC-Ka, and hClC-Kb. This is in contrast to findings from Adachi *et al.*, who reported currents with kinetics similar to rClC-K1 after expression of rClC-K2 (4). However, they observed identical currents with a rClC-K2 splice variant that completely lacked the second transmembrane domain (4). This could argue for the induction of an anion conductance endogenous to *Xenopus* oocytes. We performed the present study with two major aims. First, we aimed to prove that rClC-K1 functions as a plasma membrane chloride channel by inserting a point mutation that changes its intrinsic channel properties. Second, by constructing chimeras between these highly related proteins, we wanted to find out which protein regions are necessary for functional expression in *Xe-*

\* This work was supported by grants from the Deutsche Forschungsgemeinschaft and the Fonds der Chemischen Industrie (to T. J. J.). The costs of publication of this article were defrayed in part by the payment of page charges. This article must therefore be hereby marked "advertisement" in accordance with 18 U.S.C. Section 1734 solely to indicate this fact.

‡ To whom correspondence should be addressed: ZMNH, University of Hamburg, Martinistr. 85, D-20246 Hamburg, Germany. Fax: 49-40-42803-4839; E-mail: siegfried.waldegger@zmnh.uni-hamburg.de.

*nopus* oocytes. We generated a chimeric channel that consisted largely of hClC-Kb and showed interesting differences in channel properties. Insertion of *CLCNKB* mutations found in human Bartter's syndrome abolished or strongly reduced these currents. This suggests that Bartter's syndrome III is due to the loss of a chloride current with characteristics that differ from those of ClC-K1 currents.

#### EXPERIMENTAL PROCEDURES

**ClC-K Constructs**—rClC-K1 and rClC-K2 as well as hClC-Ka and hClC-Kb (2) were cloned into pTLN (14), a vector that contains *Xenopus* globin untranslated sequences and is optimized for protein expression in *Xenopus* oocytes. Single point mutations were introduced by recombinant polymerase chain reaction. To construct chimeras between hClC-Kb and rClC-K1, rClC-K1 cDNA segments were amplified with chimeric oligonucleotides that contained terminal overhangs corresponding to the respective hClC-Kb sequences. Two flanking hClC-Kb sequences were amplified in separate reactions. These three amplification products were joined by a single recombinant polymerase chain reaction, digested with appropriate restriction endonucleases, and ligated into the cut hClC-Kb/pTLN construct. All polymerase chain reaction-derived fragments were entirely sequenced.

**Expression in *Xenopus laevis* Oocytes and Voltage Clamp Analysis**—SP6 polymerase (mMessage mMachine kit; Ambion) was used for *in vitro* transcription of capped cRNA after linearization of the constructs with *Mlu*I. 10 ng of cRNA was injected in defolliculated oocytes. Oocytes were kept at 17 °C in ND96 solution containing 96 mM NaCl, 2 mM KCl, 1.8 mM CaCl<sub>2</sub>, 1 mM MgCl<sub>2</sub>, 5 mM HEPES (pH 7.4), and gentamycin (20 μg/ml). 2–3 days after injection, two-electrode voltage clamp measurements were performed at room temperature with a Turbotec 05 amplifier (NPI Instruments) and pClamp 5.5 software (Axon Instruments). Currents were recorded in ND96 solution (without gentamycin). For anion replacement experiments, 80 mM chloride was substituted by equivalent amounts of bromide, iodide, or nitrate. Anion permeability ratios were calculated using the modified Goldman equation,

$$P_{(\text{anion})}/P_{(\text{chloride})} = (104 \times e^{40 \times (E1 - E2)} - 24)/80 \quad (\text{Eq. 1})$$

where *E1* and *E2* correspond to the reversal potentials (in volts) before and after substitution of 80 mM chloride by the indicated anions, respectively. The relative anion conductance sequences were determined from the current amplitudes at +60 mV in the presence of ND96 or after replacement of 80 mM chloride by the respective anions. Statistic values are presented as mean ± S.E. (*n* represents the number of experiments).

When using different pH values, 5 mM HEPES (for pH 7.0 and 7.5) was replaced by 5 mM MES<sup>1</sup> (for pH 5.0–6.5) or 5 mM TRIS (pH 8.0). Extracellular divalent cation concentration was varied by adding calcium acetate or magnesium acetate to the ND96 solution.

**Surface Biotinylation and Western Blot Analysis**—A membrane-impermeable NH<sub>2</sub>-reactive biotin ester (sulfo-*N*-hydroxysuccinimide-LC-biotin; Pierce) was used to label plasma membrane proteins of *Xenopus* oocytes expressing ClC-K constructs. Oocytes were incubated for 10 min at room temperature in ND96 with a 0.5 mg/ml concentration of the biotin ester. After several washes in ice-cold ND96, the cells were homogenized in lysis buffer containing 150 mM NaCl, 20 mM Tris (pH 7.6), 1% Triton X-100, and a protease inhibitor mixture (Complete; Roche Molecular Biochemicals). Insoluble material was separated by centrifugation, and the clear supernatant was precipitated with streptavidin beads (Pierce). The precipitate was separated on a 10% SDS-polyacrylamide gel. For Western blot analysis, we used a rat monoclonal antibody (3F10; 200 ng/ml; Roche Molecular Biochemicals) directed against an HA epitope we had added to the amino terminus of the ClC-K constructs. Primary and secondary (horseradish peroxidase-conjugated goat anti-rat IgG, 1:10,000) antibodies were diluted in TBS (150 mM NaCl, 25 mM Tris, pH 7.4) containing 5% nonfat milk powder and 0.1% Tween 20. Reacting proteins were detected with the Renaissance reagent (NEN Life Science Products) and photographic film (Eastman Kodak Co.).

#### RESULTS

We cloned the rClC-K1 cDNA into an optimized expression vector containing the 5'- and 3'-untranslated regions of the *Xenopus* β-globin gene. Two to three days after injecting cRNA

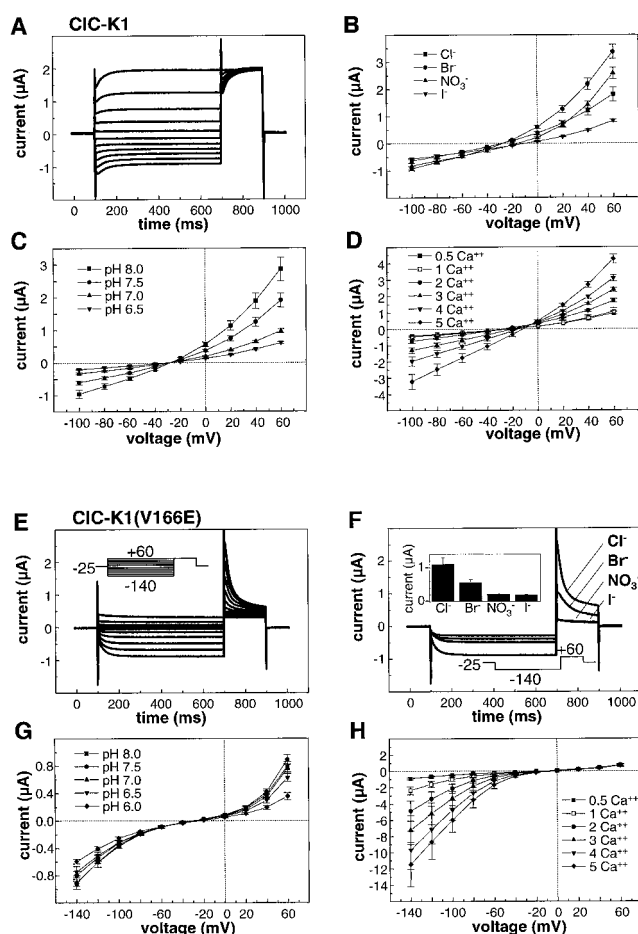


**FIG. 1. Functional expression of rClC-K1 in *Xenopus* oocytes.** A, current traces of wild type rClC-K1. Currents were measured in ND96 with the voltage clamp protocol indicated in E. B, I-V relationships of rClC-K1 currents. 80 mM extracellular chloride was substituted by the indicated anions (*n* = 10). rClC-K1-induced currents are shown at different extracellular pH values (*n* = 7) (C) and calcium concentrations (indicated in mM; *n* = 7) (D). E, current traces of rClC-K1(V166E) measured in ND96. F, amplitude of rClC-K1(V166E) tail currents measured at +60 mV and statistical analysis of maximal tail current amplitudes (*n* = 5). G, I-V relationships of rClC-K1(V166E)-induced currents at different extracellular pH values (*n* = 7) and calcium concentrations (*n* = 5) (H).

derived from this construct into *Xenopus* oocytes, two-electrode voltage clamp measurements revealed nearly instantaneous, slightly outwardly rectifying currents. They showed some time-dependent gating at voltages more positive than +40 mV or more negative than -100 mV (Fig. 1A). Partial replacement of extracellular chloride by other anions indicated a  $\text{Br}^- > \text{NO}_3^- \geq \text{Cl}^- > \text{I}^-$  conductance sequence (Fig. 1B). Reversal potential measurements upon substitution of 80 mmol/liter Cl<sup>-</sup> with different anions revealed an anion permeability sequence of  $\text{Cl}^- > \text{Br}^- > \text{NO}_3^- > \text{I}^-$  (Table I). The current amplitude increased upon extracellular alkalization to pH 8.0 and strongly decreased when the extracellular pH was reduced from pH 7.5 to pH 6.5 (Fig. 1C). These properties were similar to those previously reported by Uchida *et al.* (7). Again similar to that study, current amplitudes were rather low (~1 μA at +60 mV) and thus difficult to discriminate from endogenous oocyte chloride currents. Although these endogenous currents display an  $\text{I}^- > \text{Cl}^-$  conductance and are not sensitive to ambient pH changes, we sought more definitive evidence that the current seen upon rClC-K1 expression is directly due to the heterologously expressed protein.

Since rClC-K1-induced currents decreased upon removal of

<sup>1</sup> The abbreviation used is: MES, 4-morpholineethanesulfonic acid.

TABLE I  
Anion permeability ( $P$ ) ratios of ClC-K1 and chimeric ClC-K constructs

Using the Goldman equation (see "Experimental Procedures") the ratios were calculated from reversal potential shift measurements (given in parenthesis) after substitution of 80 mM chloride with the indicated anions. The constructs ClC-K1(D2)Kb(D5)K1 and ClC-K1(D1)Kb(D5)K1 refer to Fig. 3, A and E, respectively.

	$P(\text{Br}^-)/P(\text{Cl}^-)$	$P(\text{NO}_3^-)/P(\text{Cl}^-)$	$P(\text{I}^-)/P(\text{Cl}^-)$
ClC-K1 ( $n = 9$ )	$0.85 \pm 0.02$ ( $2.6 \pm 0.9$ mV)	$0.47 \pm 0.01$ ( $12.3 \pm 0.7$ mV)	$0.33 \pm 0.04$ ( $17.9 \pm 2.3$ mV)
ClC-Kb(D4)K1 ( $n = 5$ )	$0.71 \pm 0.05$ ( $5.8 \pm 1.7$ mV)	$0.16 \pm 0.03$ ( $25.9 \pm 2.3$ mV)	$0.12 \pm 0.03$ ( $28.0 \pm 2.1$ mV)
ClC-Kb(D5)K1 ( $n = 5$ )	$0.76 \pm 0.04$ ( $5.0 \pm 1.4$ mV)	$0.24 \pm 0.04$ ( $21.3 \pm 2.4$ mV)	$0.14 \pm 0.03$ ( $26.1 \pm 2.2$ mV)
ClC-K1(D2)Kb(D5)K1 ( $n = 5$ )	$0.90 \pm 0.02$ ( $2.0 \pm 0.4$ mV)	$0.22 \pm 0.03$ ( $22.4 \pm 1.0$ mV)	$0.14 \pm 0.01$ ( $26.4 \pm 1.2$ mV)
ClC-K1(D1)Kb(D5)K1 ( $n = 5$ )	$0.72 \pm 0.04$ ( $5.4 \pm 1.3$ mV)	$0.12 \pm 0.02$ ( $28.0 \pm 1.9$ mV)	$0.09 \pm 0.02$ ( $29.4 \pm 1.5$ mV)
ClC-Kb(c) ( $n = 7$ )	$0.61 \pm 0.01$ ( $9.7 \pm 1.0$ mV)	$0.05 \pm 0.02$ ( $32.9 \pm 2.3$ mV)	$0.16 \pm 0.01$ ( $25.9 \pm 1.6$ mV)
ClC-Kb(c)(V166E) ( $n = 7$ )	$0.54 \pm 0.01$ ( $10.6 \pm 0.7$ mV)	$0.36 \pm 0.01$ ( $16.4 \pm 0.7$ mV)	$0.31 \pm 0.03$ ( $18.6 \pm 1.7$ mV)

extracellular calcium (7), we investigated whether we could increase currents by raising the extracellular concentration of divalent cations. Whereas the addition of 5 mM magnesium or barium had no appreciable effect (data not shown), the elevation of extracellular calcium concentration from 1 to 5 mM increased current amplitudes nearly 4-fold (Fig. 1D). This increase occurred immediately after bath fluid exchange and was rapidly reversible upon wash-out. This points to an extracellular effect of calcium. The anion conductance sequence and the pH sensitivity of rClC-K1 currents were not affected by this maneuver (data not shown). This effect clearly distinguished rClC-K1 currents from endogenous oocyte currents particularly as elevation of extracellular calcium concentration to 5 mM failed to induce an anion conductance in uninjected oocytes or oocytes injected with cRNAs derived from hClC-Kb, hClC-Ka, or rClC-K2 (data not shown).

To show more directly that rClC-K1 functions as a chloride channel, we sought to change key biophysical properties (like ion selectivity or gating) by a point mutation. Mutations in a highly conserved motif (GKEGP) at the end of the third transmembrane domain (D3) are known to change gating and pore properties of several CLC channels (15–18). Interestingly, the glutamate in this motif is exchanged for a hydrophobic amino acid (valine or leucine) in all known ClC-K proteins. We mutated this valine to glutamate in rClC-K1 (V166E) and thus converted this region to the GKEGP consensus sequence found in all other members of the CLC family. This mutation changed rClC-K1 gating drastically (Fig. 1E). Instead of the rather voltage-independent gating of wild type rClC-K1, currents now activated slowly upon hyperpolarization. Additionally, measurements of tail currents in the presence of different anions revealed that the V166E mutation changed the anion conductance sequence from  $\text{Br}^- > \text{NO}_3^- \geq \text{Cl}^- > \text{I}^-$  (wild type) to  $\text{Cl}^- > \text{Br}^- > \text{NO}_3^- = \text{I}^-$  (Fig. 1F). Similar to wild type currents, lowering extracellular pH decreased, and raising extracellular calcium concentration increased current amplitudes (Fig. 1, G and H). Niflumic acid (10  $\mu\text{M}$ ) and anthracene-9-carboxylic acid (500  $\mu\text{M}$ ) had no effect, whereas 4,4'-diisothiocyanostilbene-2,2'-disulfonic acid (500  $\mu\text{M}$ ) completely blocked currents induced by both wild type ClC-K1 and ClC-K1(V166E) (data not shown).

Having demonstrated that rClC-K1 directly mediates anion currents, we expressed rClC-K2, hClC-Ka, and hClC-Kb in *Xenopus* oocytes, using the same efficient oocyte expression vector. In contrast to Adachi *et al.* (4), who reported that rClC-K2 induced currents in *Xenopus* oocytes, we could not detect anion currents above background with any of these constructs. This is surprising, since they are roughly 90% iden-

tical to rClC-K1 (Fig. 2A). To identify protein regions that may be necessary for the functional expression of hClC-Kb, we replaced several regions of this protein with the corresponding stretches derived from rClC-K1. These constructs were named according to the sequential order of the individual components (from the N terminus to the C terminus). The region in parenthesis indicates the position where these were fused together. Thus, ClC-K1(D9)Kb denotes a chimera in which an amino-terminal rClC-K1 stretch is fused to a carboxyl-terminal hClC-Kb sequence within transmembrane domain D9 (according to the topology model published in Ref. 18). None of the chimeras in which amino-terminal portions of hClC-Kb were replaced with the corresponding rClC-K1 sequences induced chloride currents in *Xenopus* oocytes (up to transmembrane region D9 (ClC-K1(D3)Kb, ClC-K1(D6)Kb, ClC-K1(D9)Kb); data not shown). By contrast, when C-terminal parts of hClC-Kb were replaced by rClC-K1 segments, we detected two different types of currents depending on the extent of the replacement. As expected, when the major part of the chimeric channel consisted of rClC-K1 (constructs ClC-Kb(D3)K1 and ClC-Kb(D4)K1), currents resembled those of rClC-K1 (Fig. 2B). This included the  $\text{Br}^- > \text{Cl}^- > \text{I}^-$  conductance sequence and the residual voltage-dependent gating at positive voltages. Surprisingly, shifting the ClC-Kb/K1 fusion point 43 amino acids further to the C terminus (ClC-Kb(D5)K1) yielded a new type of current (Fig. 2C). The current amplitude increased about 10-fold, the conductance sequence was changed to  $\text{Cl}^- > \text{Br}^- > \text{I}^-$ , and there was no obvious voltage-dependent gating even at rather positive voltages. As indicated in Table I, the permeability sequence of  $\text{Cl}^- > \text{Br}^- > \text{NO}_3^- \geq \text{I}^-$  did not change. Similar currents were observed with a successive reduction of the rClC-K1 portion with constructs ClC-Kb(D6)K1, ClC-Kb(D7)K1, ClC-Kb(D8)K1, and ClC-Kb(D9)K1 (Fig. 2D). However, current amplitudes gradually decreased in parallel to the replacement of rClC-K1 with hClC-Kb sequences (Fig. 2E).

The drastic alteration in channel properties observed upon shifting the fusion point from the beginning of D4 to the beginning of D5 suggested an involvement of the D4 domain in determining anion conductivity properties and gating. To test whether the changes in channel properties are solely due to the exchange of the D4 domain, we engineered several rClC-K1 constructs in which D4 alone or together with adjacent protein regions were replaced with the corresponding hClC-Kb regions. In contrast to the expectation, exchanging the D4 domain of rClC-K1 with that of hClC-Kb, either alone (data not shown) or together with D3 and a portion of D2 (Fig. 3A), resulted in a similar anion conductance sequence (Fig. 3, B and C) or pH and calcium sensitivity (Fig. 3D) as observed for rClC-K1. However,

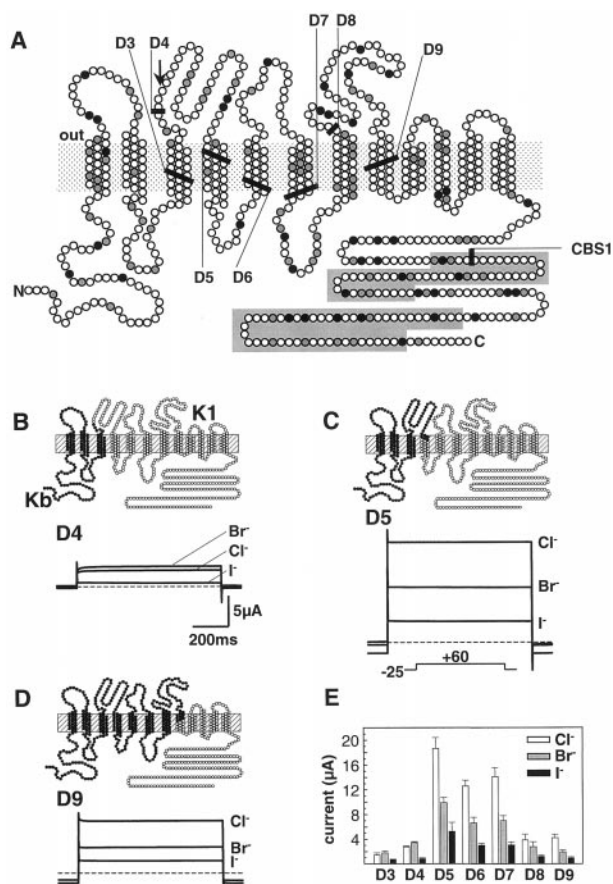


**FIG. 2. Functional analysis of ClC-Kb/CIC-K1 chimeric channel constructs expressed in *Xenopus oocytes*.** *A*, ClC-K topology model indicating identical amino acids (*white*) as well as conserved (*gray*) and nonconserved (*black*) amino acid exchanges between hClC-Kb and rClC-K1. The *black bars* mark the fusion points of the various chimeric channel constructs. The *arrow* at the D4 domain indicates the amino acid position 166 mutated in rClC-K1 an hClC-Kb(c) (see Figs. 1 and 4). The two C-terminal CBS domains (19) are *highlighted*. Current traces in the presence of ND96 ( $Cl^-$ ) and after substitution of 80 mM  $Cl^-$  by  $Br^-$  and  $I^-$  are shown for the constructs ClC-Kb(D4)K1 (*B*), ClC-Kb(D5)K1 (*C*), and ClC-Kb(D9)K1 (*D*) (the *broken line* indicates the zero current level). *Black* and *white circles* indicate the hClC-Kb (*Kb*) and rClC-K1 (*K1*) portion, respectively. *E*, statistical analysis of current amplitudes measured at +60 mV throughout the constructs ClC-Kb(D3)K–ClC-Kb(D9)K1. Current amplitudes were determined from more than five oocytes per construct.

these properties changed after transplanting a larger hClC-Kb protein region that comprised the C-terminal part of D1 and the N-terminal part of D5 (Fig. 3*E*). Besides a  $Cl^- > Br^- > I^-$  conductance sequence (Fig. 3, *F* and *G*), this construct showed a reduced sensitivity toward extracellular acidification to pH 6.5 (Fig. 3*H*). In addition, the elevation of extracellular calcium concentration had only a small effect on current amplitudes (Fig. 3*H*). As evident from Table I, the anion permeability sequences of both constructs were nearly identical.

Extending the hClC-Kb portion further toward the carboxyl terminus beyond the transmembrane block D9–D12 did not result in functional channels (data not shown). To obtain a functional construct that contained a larger portion of hClC-Kb, we replaced progressively larger parts of the ClC-Kb(D9)K1 C terminus with stretches derived from hClC-Kb. A total exchange of the intracellular C terminus, however, resulted in a construct that did not yield currents (data not shown). In contrast, a partial replacement (with the fusion point within the CBS1 domain (19–21)) yielded currents that resembled those of ClC-Kb(D9)K1. As we could not reduce

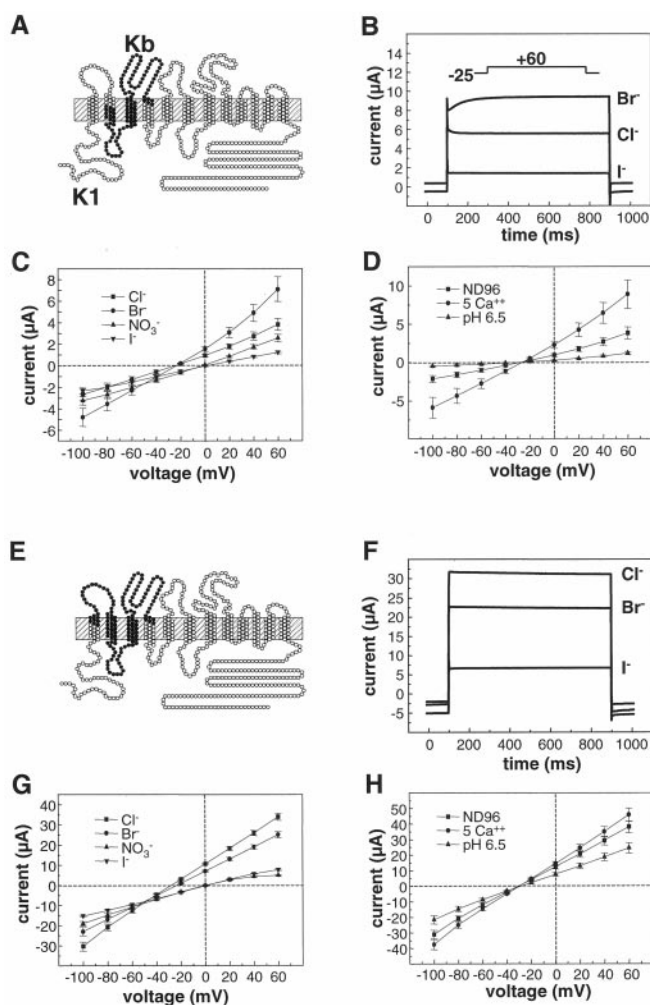


**FIG. 3. Identification of the protein region responsible for the functional differences between ClC-Kb(D4)K1 and ClC-Kb(D5)K1.** hClC-Kb derived protein regions (*black circles*) were transferred to rClC-K1 (*white circles*) as indicated in the channel models (*A* and *E*). *B* and *F*, current traces in the presence of ND96 ( $Cl^-$ ) and after substitution of 80 mM  $Cl^-$  by  $Br^-$  and  $I^-$ . *C* and *G*, *I-V* relationships after substitution of 80 mM  $Cl^-$  by  $Br^-$ ,  $I^-$ , and  $NO_3^-$ . *D* and *H*, *I-V* relationships under control conditions (ND96), at an extracellular pH of 6.5, and after increase of extracellular calcium concentration to 5 mM. The segment boundaries were as follows (amino acid positions): 88–207 (*A*), and 56–207 (*E*).

further the contribution of rClC-K1 sequences without losing functional expression, we used this construct to further characterize channel properties. We named this construct ClC-Kb(c) (where “c” represents chimeric).

Expression of ClC-Kb(c) in *Xenopus oocytes* gave rise to linear currents with no appreciable voltage dependence (Fig. 4*A*). The shift of the reversal potential of about 53 mV per decade of change of extracellular chloride concentration pointed to a selective chloride conductance (Fig. 4*B*). As expected for a chloride current, the reversal potential was close to  $-30$  mV (Fig. 4*C*). Anion replacement experiments revealed a  $Cl^- > Br^- > I^- > NO_3^-$  conductance sequence (Fig. 4*C*). The shift in reversal potential indicated a similar permeability sequence (Table I). Comparable with rClC-K1, ClC-Kb(c)-induced currents decreased upon extracellular acidification (Fig. 4*D*). With the half-maximal inhibition occurring at pH 6.3, the pH sensitivity was shifted to more acidic pH values as compared with rClC-K1. Similar to rClC-K1, the V166E mutation conferred voltage dependence on ClC-Kb(c)-induced currents (Fig. 4*E*). In contrast to the rClC-K1(V166E) mutation, however,

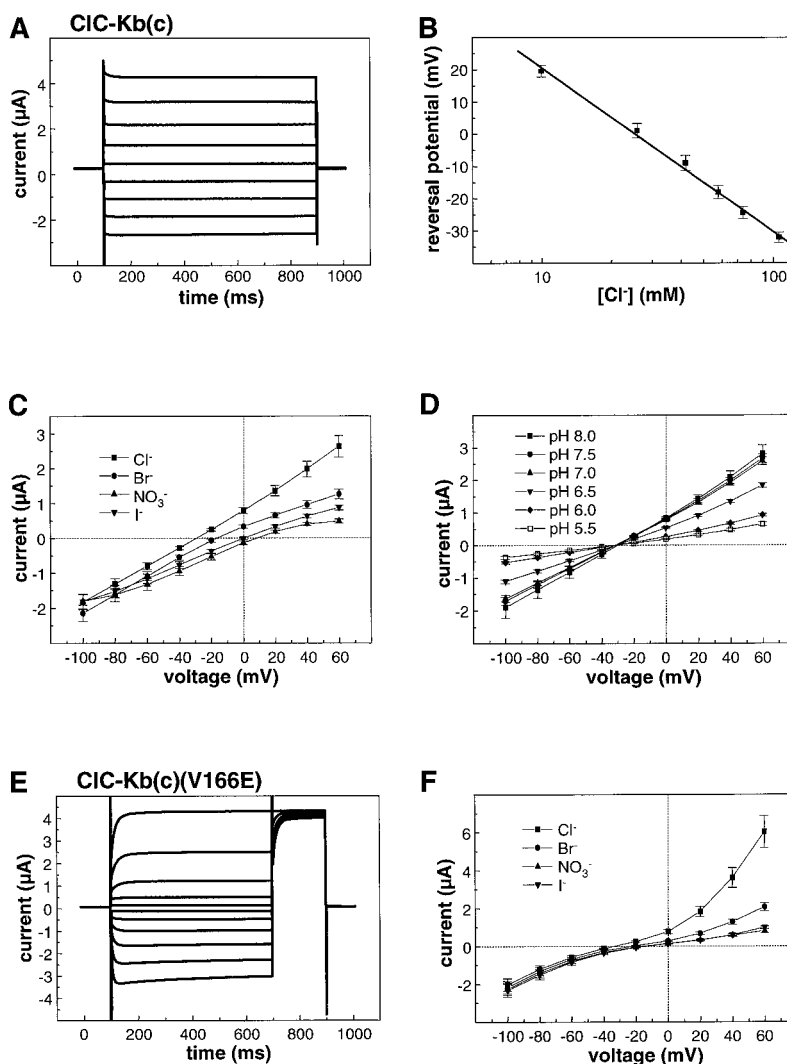


FIG. 4. Functional characteristics of ClC-Kb(c) currents in *Xenopus* oocytes. *A*, current traces recorded in ND96 with the voltage clamp protocol shown in Fig. 5*A*. *B*, reversal potential shift in dependence of extracellular chloride concentration after equimolar substitution of chloride by aspartate ( $n = 5$ ). *C*, *I*-*V* relationships of ClC-Kb(c) currents in the presence of ND96 ( $\text{Cl}^-$ ) and after substitution of 80 mM  $\text{Cl}^-$  by  $\text{Br}^-$ ,  $\text{NO}_3^-$ , and  $\text{I}^-$  ( $n = 7$ ). *D*, pH dependence of ClC-Kb(c)-induced currents. *E*, currents measured after expression of ClC-Kb(c)(V166E). *F*, *I*-*V* relationships of ClC-Kb(c)(V166E)-induced currents under anionic conditions as described for *C*.

these currents were activated not only at negative voltages but also in the positive voltage range and no significant tail currents could be observed (Fig. 4, *E* and *F*). Moreover, the anion conductance sequence was not affected by this mutation (Fig. 4*F*). An increase in extracellular calcium concentration did not change the magnitude of ClC-Kb(c) and ClC-Kb(c)(V166E)-mediated currents (data not shown).

Because hClC-Kb could not be expressed functionally, it has not yet been possible to analyze the biophysical consequences of *CLCNKB* mutations associated with Bartter's syndrome. We therefore introduced the point mutations that were found in patients (11) into the ClC-Kb(c) construct (P124L, A204T, A349D, Y432H, and R438C) and expressed these in oocytes. Invariably these mutations either strongly reduced (Y432H) or completely abolished ClC-Kb(c) currents (Fig. 5*A*). In order to determine the level of expression of these proteins, they were tagged with an HA epitope at the amino terminus. After labeling the plasma membrane proteins externally with biotin, we performed Western blot analysis of total cellular lysates and of the purified biotin-labeled protein fractions. Immunodetection with an anti-HA antibody demonstrated that the mutated ClC-Kb(c) constructs were efficiently translated and transported to the plasma membrane (Fig. 5*B*). In addition to a band of the predicted molecular size (80 kDa), a more prominent band appeared at about 160 kDa, which may be due to a dimerization of the ClC-K proteins. As is also evident from Fig. 5*B*, the HA-tagged version of the wild type hClC-Kb protein showed a

similar degree of biotin labeling as the ClC-Kb(c) construct. Wild type hClC-Kb hence seemed to reach the plasma membrane.

#### DISCUSSION

ClC-K channels have attracted considerable interest because of their importance in renal physiology. Mutations in genes encoding ClC-K channels result in Bartter's syndrome and in nephrogenic diabetes insipidus. Based on these findings and on the localization of the corresponding mRNAs and proteins in certain segments of the nephron, it was proposed that ClC-K channels are involved in transepithelial transport. Unfortunately, however, no functional expression could be obtained so far for the hClC-Ka and hClC-Kb channels, and data for the rClC-K1 and rClC-K2 were controversial. A correlation with channels found *in situ* and an investigation of the physiological consequences of mutations found in Bartter's syndrome, however, requires data on the functional properties of these channels.

We now demonstrate that expression of rClC-K1 in *Xenopus* oocytes induces currents similar to those described by Uchida *et al.* (7). However, rather similar currents but with an  $\text{I}^- > \text{Cl}^-$  conductance were reported by the same group for rClC-K2 and a rClC-K2 splice variant that lacks the second transmembrane domain (4). Since it is rather unlikely that the deletion of a complete transmembrane domain has no impact on channel function, we were worried that these currents were mediated

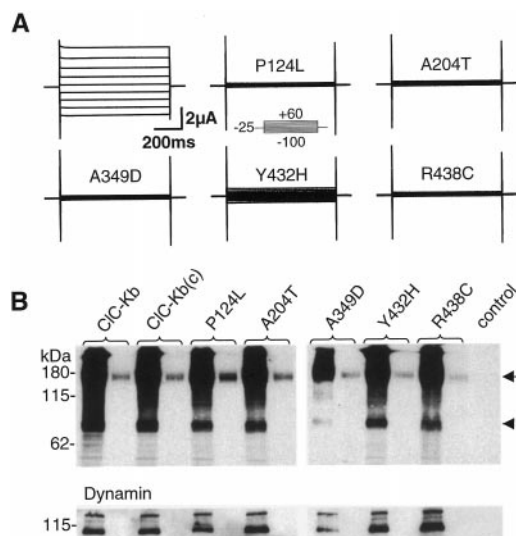


**FIG. 5. Functional consequences of point mutations associated with Bartter's syndrome type III on CLC-Kb(c).** *A*, current traces of CLC-Kb(c) (upper left) and of CLC-Kb(c) carrying the indicated point mutations. *B*, Western blot analysis of hCLC-Kb and CLC-Kb(c) constructs expressed in *Xenopus* oocytes. The same oocytes were used as in *A*. For detection, a HA epitope was added to the N terminus of the different constructs, which allowed the detection by a monoclonal anti-HA antibody. Total cellular lysates (left lane) and the biotinylated membrane protein fraction (right lane) were separated on a 10% SDS-polyacrylamide gel. The arrowhead indicates the protein band with the calculated molecular mass (80 kDa). The 160-kDa band (indicated by the arrow) is probably due to a dimerization of the proteins. The biotinylated membrane protein fraction of oocytes expressing CLC-Kb(c) without HA epitope served as control. Reprobing of the same blot with an anti-dynamin antibody (lower panel) demonstrates the absence of biotinylation of membrane-associated intracellular dynamin.

by an activation of channels endogenous to oocytes. Indeed, the injection of cRNAs encoding diverse proteins can induce several distinct anion conductances that are endogenous to *Xenopus* oocytes (22). Consequently, one has to be very cautious when studying newly expressed chloride currents in oocytes or other expression systems.

Mutations that influence biophysical properties suggest very strongly that the mutated protein is indeed an ion channel. To find such a mutation, we focused on a region that is known to influence gating and conductance in other CLC proteins. We could show that a single point mutation in this region (V166E) changes both the anion conductance sequence and gating of rCLC-K1-mediated currents. This demonstrates unambiguously that rCLC-K1 directly mediates plasma membrane currents.

The V166E mutation restores the GKEGP consensus sequence found in all other known CLC proteins and introduces a strong voltage-dependent gating. Interestingly, when the naturally occurring glutamate of the GKEGP motif was neutralized to alanine in the CLC-4 and CLC-5 chloride channels, their strong outward rectification was abolished (23). Although there is no simple conclusion (the voltage-dependence of wild type CLC-4 and CLC-5 is just opposite to that of the rCLC-K1 mutant that shares the glutamate in the GKEGP motif), this indicates that this segment is somehow important for gating (although it is unlikely to form a voltage sensor). It seems that CLC-K channels have largely lost their voltage-dependent gating by inserting a neutral amino acid at this position. This may be important for their role in transepithelial transport.

The stretch between D3 and D4, which encompasses the conserved GKEGP sequence, is known from several studies to somehow influence ion selectivity and gating of other CLC channels (15–18, 23, 24), and it has been suggested (16) that

this segment directly lines the pore. At first, our chimeric experiments seemed to support this simple concept; when the borders between hCLC-Kb and rCLC-K1 were shifted in such a way as to include the D4 domain of hCLC-Kb, we observed quite drastic changes in the anion conductance sequence and gating. These changes, however, cannot be explained by a difference in the GKVG motif, since it is identical in both channels. More important, transplantations of D4 and adjacent regions from hCLC-Kb into rCLC-K1 only induced biophysical changes if the exchanged region also included parts of the D1 region. Thus, at least with CLC-K channels, pore properties cannot be transferred by simply transplanting a short segment containing D3–D4 as has been previously reported for CLC-1/CLC-3 chimeras (16). Indeed, point mutations in several protein regions (e.g. between D2 and D3 and at the end of D12) were previously shown to change pore properties (25–28). This is not astonishing, because in these ion channels an ion conductive pore is probably formed by a single protein subunit. CLC-0 and CLC-1 are dimers with two quite independent pores (26, 27, 29), suggesting one pore per subunit (but see Ref. 30). The present data indicate that changes in ion conductivity even between structurally highly related channels may require the coordinate mutation of residues that are not close to each other in the linear primary structure.

In contrast to rCLC-K1, we could not detect chloride currents after expression of rCLC-K2, hCLC-Ka, and hCLC-Kb. Rabbit CLC-Ka (5) and xCLC-K from *Xenopus* (6) were also reported not to give rise to currents, and the currents reported for rCLC-K2 (4) might be due to currents endogenous to *Xenopus* oocytes. It is currently unclear why, with the exception of rCLC-K1, most CLC-K protein do not yield currents upon heterologous expression. This is puzzling given the very high degree of homology between these proteins. We succeeded in engineering a functional chimera that contains mostly sequences that are derived from hCLC-Kb and has distinct functional properties. This shows that, in the framework of the chimera, the hydrophobic D9–D12 block is necessary for functional expression. However, it does not give any clue as to why this segment enables expression. Although several CLC channels probably function in intracellular organelles (21, 31, 32), the likely function of CLC-K channels in transepithelial transport, together with immunohistochemical studies (7–9), suggests that this is not the case for CLC-K channels *in vivo*. Further, our surface biotinylation experiments show that these proteins reach the plasma membrane to some degree also in our expression system. Thus, we are left with the following two other main possibilities: although no  $\beta$ -subunit is currently known for any CLC channel, such an accessory protein may be necessary for functional expression; alternatively, there may be a need for a second messenger that we have not yet tested. However, even if one of these hypotheses is true, it remains enigmatic that we could not see currents with any of the human channels, because one of these (probably hCLC-Ka) should be the direct species homologue of rCLC-K1, which does give currents.

We have constructed a functional chimera that consists largely of hCLC-Kb, but contains the D9–D12 stretch from rCLC-K1. We could not reduce the proportion of rCLC-K1 further without losing current. This chimera yielded currents that were distinctly different from those of rCLC-K1. These properties remained qualitatively unchanged when the fusion point was shifted between the end of D4 and the end of D9. However, we cannot be sure that the biophysical properties of the CLC-Kb(c) construct represent those of native hCLC-Kb channels. Indeed, many point mutations in the D9–D12 region are known to affect properties of several CLC channels (15, 18, 24, 25, 33, 34).

Nonetheless, it is tempting to speculate that the changed properties of this current (voltage dependence, anion conductance sequence, and lack of an effect of extracellular calcium) reflect the properties of native hClC-Kb channels. Chloride channels with an anion selectivity similar to ClC-Kb(c) were described in the basolateral membrane of thick ascending limb cells (35, 36). In a more indirect approach, Winters *et al.* demonstrated the appearance of an anion conductance with a  $\text{Cl}^- > \text{I}^-$  selectivity in lipid bilayers after fusion with basolaterally enriched vesicles from rabbit outer kidney medulla (37). Taken together, these findings suggest that ClC-Kb(c) type currents are mirrored *in situ* at the basolateral membrane of thick ascending limb cells. Importantly, this construct also allowed us for the first time to test the biophysical effects of point mutations found in Bartter's syndrome (11). All missense mutations either abolished or strongly reduced these currents. This is consistent with the finding that many CLCNKB mutations in Bartter's syndrome are total or partial gene deletions (11), which will invariably abolish channel activity.

Chloride transport in the thin ascending limb of Henle's loop was shown to depend on ambient calcium concentration (38). This is consistent with the finding that heterologously expressed ClC-K1 is activated by extracellular calcium. This activation occurs within the physiological range of calcium concentrations observed in the tubular lumen of Henle's loop (39). However, changes in tubular and interstitial calcium concentrations affect a variety of transport processes in different nephron segments (40–42); thus, the functional relevance of this effect is difficult to predict. A comparable effect of extracellular calcium was not described for any of the other members of the ClC chloride channel family. It therefore remains to be determined in patch clamp experiments whether the increase in rClC-K1 current amplitude is due to an increase in single channel conductance or in open probability of rClC-K1 channels.

In summary, the functional characteristics of rClC-K1-mediated currents harmonize with macroscopic currents described in isolated thin ascending limbs. This applies to their voltage dependence, ion selectivity, and sensitivity to changes in ambient pH and calcium concentration. Currents similar to those mediated by ClC-Kb(c) were identified in the basolateral membrane of the thick ascending limb. Moreover, Bartter's syndrome-associated mutations in the CLCNKB gene destroy ion channel function of ClC-Kb(c).

*Acknowledgments*—We thank Mirko Hechenberger for critical reading of the manuscript and Holger Slamal for technical assistance.

#### REFERENCES

- Jentsch, T. J., Friedrich, T., Schriever, A., and Yamada, H. (1999) *Pflügers Arch. Eur. J. Physiol.* **437**, 783–795
- Kieferle, S., Fong, P., Bens, M., Vandewalle, A., and Jentsch, T. J. (1994) *Proc. Natl. Acad. Sci. U. S. A.* **91**, 6943–6947
- Uchida, S., Sasaki, S., Furukawa, T., Hiraoka, M., Imai, T., Hirata, Y., and Marumo, F. (1993) *J. Biol. Chem.* **268**, 3821–3824
- Adachi, S., Uchida, S., Ito, H., Hata, M., Hiroe, M., Marumo, F., and Sasaki, S. (1994) *J. Biol. Chem.* **269**, 17677–17683
- Zimniak, L., Winters, C. J., Reeves, W. B., and Andreoli, T. E. (1995) *Kidney Int.* **48**, 1828–1836
- Maulet, Y., Lambert, R. C., Mykita, S., Mouton, J., Partisani, M., Bailly, Y., Bombarde, G., and Feltz, A. (1999) *Biochem. J.* **340**, 737–743
- Uchida, S., Sasaki, S., Nitta, K., Uchida, K., Horita, S., Nihei, H., and Marumo, F. (1995) *J. Clin. Invest.* **95**, 104–113
- Vandewalle, A., Cluzeaud, F., Bens, M., Kieferle, S., Steinmeyer, K., and Jentsch, T. J. (1997) *Am. J. Physiol.* **272**, F678–F688
- Winters, C. J., Zimniak, L., Reeves, W. B., and Andreoli, T. E. (1997) *Am. J. Physiol.* **273**, F1030–F1038
- Matsumura, Y., Uchida, S., Kondo, Y., Miyazaki, H., Ko, S. B. H., Hayama, A., Morimoto, T., Liu, W., Arisawa, M., Sasaki, S., and Marumo, F. (1999) *Nat. Genet.* **21**, 95–98
- Simon, D. B., Bindra, R. S., Mansfield, T. A., Nelson-Williams, C., Mendonca, E., Stone, R., Schurman, S., Nayir, A., Alpay, H., Bakkaloglu, A., Rodriguez-Soriano, J., Morales, J. M., Sanjad, S. A., Taylor, C. M., Pilz, D., Brem, A., Trachtman, H., Griswold, W., Richard, G. A., John, E., and Lifton, R. P. (1997) *Nat. Genet.* **17**, 171–178
- Simon, D. B., Karet, F. E., Hamdan, J. M., Di Pietro, A., Sanjad, S. A., and Lifton, R. P. (1996) *Nat. Genet.* **13**, 183–188
- Simon, D. B., Karet, F. E., Rodriguez-Soriano, J., Hamdan, J. H., DiPietro, A., Trachtman, H., Sanjad, S. A., and Lifton, R. P. (1996) *Nat. Genet.* **14**, 152–156
- Lorenz, C., Pusch, M., and Jentsch, T. J. (1996) *Proc. Natl. Acad. Sci. U. S. A.* **93**, 13362–13366
- Steinmeyer, K., Lorenz, C., Pusch, M., Koch, M. C., and Jentsch, T. J. (1994) *EMBO J.* **13**, 737–743
- Fahlke, C., Yu, H. T., Beck, C. L., Rhodes, T. H., and George, A. L. J. (1997) *Nature* **390**, 529–532
- Fahlke, C., Beck, C. L., and George, A. L. (1997) *Proc. Natl. Acad. Sci. U. S. A.* **94**, 2729–2734
- Schmidt-Rose, T., and Jentsch, T. J. (1997) *Proc. Natl. Acad. Sci. U. S. A.* **94**, 7633–7638
- Ponting, C. P. (1997) *Mol. Med.* **75**, 160–163
- Schmidt-Rose, T., and Jentsch, T. J. (1997) *J. Biol. Chem.* **272**, 20515–20521
- Schwappach, B., Stobrawa, S., Hechenberger, M., Steinmeyer, K., and Jentsch, T. J. (1998) *J. Biol. Chem.* **273**, 15110–15118
- Buyse, G., Voets, T., Tytgat, J., De Greef, C., Droogmans, G., Nilius, B., and Eggermont, J. (1997) *J. Biol. Chem.* **272**, 3615–3621
- Friedrich, T., Breiderhoff, T., and Jentsch, T. J. (1999) *J. Biol. Chem.* **274**, 896–902
- Ludewig, U., Jentsch, T. J., and Pusch, M. (1997) *J. Gen. Physiol.* **110**, 165–171
- Pusch, M., Ludewig, U., Rehfeldt, A., and Jentsch, T. J. (1995) *Nature* **373**, 527–531
- Ludewig, U., Pusch, M., and Jentsch, T. J. (1996) *Nature* **383**, 340–343
- Middleton, R. E., Pheasant, D. J., and Miller, C. (1996) *Nature* **383**, 337–340
- Ludewig, U., Jentsch, T. J., and Pusch, M. (1997) *J. Physiol. (Lond.)* **498**, 691–702
- Saviane, C., Conti, F., and Pusch, M. (1999) *J. Gen. Physiol.* **113**, 457–467
- Fahlke, C., Rhodes, T. H., Desai, R. R., and George, A. L. (1998) *Nature* **394**, 687–690
- Günther, W., Lüchow, A., Cluzeaud, F., Vandewalle, A., and Jentsch, T. J. (1998) *Proc. Natl. Acad. Sci. U. S. A.* **95**, 8075–8080
- Devuyt, O., Christie, P. T., Courtoy, P. J., Beauwens, R., and Thakker, R. V. (1999) *Hum. Mol. Genet.* **8**, 247–257
- Pusch, M., Steinmeyer, K., Koch, M. C., and Jentsch, T. J. (1995) *Neuron* **15**, 1455–1463
- Zhang, J., Sanguinetti, M. C., Kwiecinski, H., and Ptacek, L. J. (2000) *J. Biol. Chem.* **275**, 2999–3005
- Paulais, M., and Teulon, J. (1990) *J. Membr. Biol.* **113**, 253–260
- Guinamard, R., Chraïbi, A., and Teulon, J. (1995) *J. Physiol.* **485**, 97–112
- Winters, C. J., Reeves, W. B., and Andreoli, T. E. (1999) *Kidney Int.* **55**, 1444–1449
- Kondo, Y., Yoshitomi, K., and Imai, M. (1988) *Am. J. Physiol.* **254**, F232–F239
- Asplin, J. R., Mandel, N. S., and Coe, F. L. (1996) *Am. J. Physiol.* **270**, F604–F613
- Brown, E. M., and Hebert, S. C. (1995) *J. Am. Soc. Nephrol.* **6**, 1530–1540
- Hebert, S. C., Brown, E. M., and Harris, H. W. (1997) *J. Exp. Biol.* **200**, 295–302
- Sands, J. M., Naruse, M., Baum, M., Jo, I., Hebert, S. C., Brown, E. M., and Harris, H. W. (1997) *J. Clin. Invest.* **99**, 1399–1405